2018 26th Mediterranean Conference on Control and Automation (MED)
Zadar, Croatia, June 19-22, 2018

Comparison of the Control Designs of an Human Co-working Endoscope Holder

You-Ting Liao, Chin-Yuan Chen, Jia-Yush Yen, Ming-Chih Ho, Yung-Yaw Chen

Abstract— **The research addresses the design of an endoscope holding robot. The minimally invasive surgery (MIS) usually takes many doctors to work together; only one surgeon is actually performing the operation. One of the doctors is required to hold the endoscope and to point the camera at the surgical area. This research aims to design a robot to fulfill the function of this doctor to hold the endoscope in place. This paper demonstrates how to achieve the two main functions of the endoscope holders namely: to maintain the entry point into the body and to actively move away from blocking the doctor in their operation. This paper describes how to achieve these goals based on a regular six degree-of-freedom industrial robots. The control could be implemented at the different levels of control. The experimental results show that the implementation at different level of controls each has its advantages and disadvantages.**

I. Introduction

The robot assisted Minimally Invasive Surgery (MIS) is becoming popular in the medical society. One famous example is the Da Vinci robotic surgical system [1, 2]. The Da Vinci system is successful with little competition mainly due to the very demanding FDA regulation that prevented any competitors from any attempt for quick results. This barrier also led the researchers to take a slightly less demanding approach, which is the endoscope holder.

As today, there are already many research results on the robotic endoscope holder. An interesting observation among these results is that the endoscope holder, like all the MIS surgical tools, requires a mean to penetrate the patient's body. To minimize the injury, the MIS robots operate under the restricting of the single point of entrance, referred to as the "remote center of motion", into the body cavity [3]. To cope with this restriction, the existing literatures almost unanimously depended upon the mechanism design to avoid having to deal with the complex problem of robot arm motion around a fixed point [3-5], and this is the standard practice even for very recent results [6].

At this point it is also worth pointing out that the endoscope holder robot always co-exists with the surgeon. The robot has to be weak enough not to hurt the people around and yet strong enough to hold the endoscope in place. Until now we do not find many research addressing this problem. Many tried to attack this problem by using weak or flexible arms with small power actuators and operated in low speeds [7-9], and some just used human interface for the doctors to give commands [4, 8, 10].

This paper considered the possibility of using control technique to achieve the required remote center of motion based upon the regular multi-axes robot. The main reason is to provide higher degree of versatility. The hardware kinematic design can achieve the purpose of a motion center; however, the center is fixed once the kinematic configuration is determined. A multi-axes robot offers much more freedom to re-construct the operating environment. It is also possible for reconfiguration of the surgeon and robot relationship.

Robot control in an environment with kinematic and dynamic constraints has been studied extensively. The readers are referred to some very helpful review papers for the background [11]. Due to the nature of the operation, the constraints imposed upon the endoscope holder combines the kinematic and dynamic constraints and is constantly changing. The control thus requires basically two main functions: (1) the remote center of motion to maintain the location of the entry point. And, (2) the human co-working ability to move out of the way when getting into the way of the physicians. This paper proposes to use the redundant control together with the compliant control to simultaneously achieve these goals. The robot in use is a six degrees-of-freedom robot arm. There is enough motion degrees-of-freedom to maintain the robot to pass through a three degree-of-freedom position in space while leaving enough freedom for the robot arm to maneuver away for certain position in space.

Also, depending on the goal of the task, the compliance control can take the form of admittance control or impedance control [11]. For the remote center of motion, we found a way to reverse the robot kinematic calculation and maintain the center of motion. As mentioned in the abstract, we realized that

*Resrach supported by The project is supported by the Ministry of Science and Technologies, Taiwan under contract no. 104-2221-E-002-197-MY3.

The authors are all with the National Taiwan University, Taipei, 10617, Taiwan.

You-Ting Liao, Chin-Yuan Chen, Jia-Yush Yen are with the Department of Mechanical Engineering (e-mail: r03522811@ntu.edu.tw, r03522811@ntu.edu.tw, jyen@ntu.edu.tw)

Ming-Chih Ho is with the Department of Surgery (e-mail: mcho1215@ntu.edu.tw)

Yung-Yaw Chen is with the Department of Electrical Engineering (e-mail: yychen@ntu.edu.tw)

the implementation of the redundant control could be conducted in the command level or in the robot arm servo control level. We have implemented both cases and allow the comparison of the results.

II. MODELING AND THE CONTROL STRATEGY

This section provides a brief description of the control strategy.

A. The Inverse Dynamics Formulation

Consider the operating environment, the endoscope holder holds the endoscope in place to provide the required picture for the physician's reference. The endoscope holder not only holds the lens in place, but also tries to avoid getting into the way for the surgeon's operation. The goal of this research is thus to achieve surgeon co-working while holding the lens in place.

As mentioned before, the proposed first method is to apply good impedance control in the lower level and then attain the remote center of motion through a restriction in the command level. Following the convention notion for the impedance control [12], the robot dynamics is expressed as:

$$D(q)\ddot{q} + C(q,\dot{q})\dot{q} + G(q) = \tau - \tau_e \quad (1)$$

The inverse dynamic function can be expressed as:

$$\tau = f(q,\dot{q},t) \quad (2)$$

If one sets $\tau_e = 0$ to eliminate the nonlinear terms, it is possible to achieve $\ddot{q} = a_q$ where a_q could be the new system input; and the resulting control would be

$$\hat{\tau} = D(q)a_q + C(q,\dot{q})\dot{q} + G(q). \quad (3)$$

Suppose D, C, and G are known precisely, then what's left of the system becomes

$D(q)\left(a_q - \ddot{q}\right) = -\tau_e$, where $D(q)$ is invertible, and

$$\left(a_q - \ddot{q}\right) = -D^{-1}(q)\tau_e. \quad (4)$$

Design the augmented control a_q by

$$a_q = \ddot{q_d} + K_d(\dot{q_d} - \dot{q}) + K_p(q_d - q) \quad (5)$$

where $d_q \in \mathrm{R}^n$ is the desired trajectory; K_d and K_p are the $n \times n$ positive definite design parameter matrices. One can convert the closed-loop dynamics into

$$(\ddot{q_d} - \ddot{q}) + K_d(\dot{q_d} - \dot{q}) + K_p(q_d - q) = 0. \quad (6)$$

It is possible to choose K_d and K_p so that the closed-loop dynamics is globally stable.

Note that for the error $e = q - q_d$ to converge, one obvious choice of the matrices K_d and K_p is

$$K_d = diag\{2\zeta_1\omega_1 \quad \cdots \quad 2\zeta_n\omega_n\} \quad (7)$$

$$K_p = diag\{\omega_1^2 \quad \cdots \quad \omega_n^2\}. \quad (8)$$

It is important at this stage to translate the result into the earth coordinates, because that is where the measurement was based.

Consider from the operational space

$\dot{X} = J(q)\dot{q}$, the derivative gives $\ddot{X} = \dot{J}(q,\dot{q})\dot{q} + J(q)\ddot{q}$.

Choose $a_q = J^{-1}(a_x - \dot{J}\dot{q})$, and set

$a_q = J^{-1}\left(a_x - \dot{J}\dot{q}\right)$, the control torque (4) becomes

$$\tau = D(q)J^{-1}\left(a_x - \dot{J}\dot{q}\right) + C(q,\dot{q})\dot{q} + G(q) \quad (9)$$

a_x can now be used for the control.

Based on the control (10), and introduce the desired operational space trajectory X_d by inserting

$$a_x = \ddot{X}_d + K_d\left(\dot{X}_d - \dot{X}\right) + K_p(X_d - X) \quad (10)$$

K_d and K_p are again the two $n \times n$ positive definite matrices, the resultant closed-loop response becomes

$$(\ddot{X}_d - \ddot{X}) + K_d\left(\dot{X}_d - \dot{X}\right) + K_p(X_d - X) = 0. \quad (11)$$

B. The Dynamic-Based Impedance Control

The impedance of an object expressed in the frequency domain would appear as

$$F(s) = Z(s)\dot{X}_s(s) \quad (12)$$

For impedance control, set the target impedance to be

$$M(\ddot{X}_d - \ddot{X}) + B\left(\dot{X}_d - \dot{X}\right) + K(X_d - X) = F_e \quad (13)$$

where $X_d \in R^n$ is the reference trajectory, and M, B, K are the $n \times n$ symmetric positive definite inertia, damping, and stiffness matrices. Rewrite (13) into

$$\ddot{X} = \ddot{X}_d + M^{-1}[B\left(\dot{X}_d - \dot{X}\right) + K(X_d - X) - F_e] \quad (14)$$

and recall the inverse dynamics (10)

$$\tau = D(q)J^{-1}\left(a_x - \dot{J}\dot{q}\right) + C(q,\dot{q})\dot{q} + G(q)$$

Back substitute to obtain

$$\tau = D(q)J^{-1}\left[\ddot{X}_d + M^{-1}\left(B\dot{E} + KE - F_e\right) - \dot{J}\dot{q}\right] \quad (15)$$

$$+h(q,\dot{q}) + J^T F_e$$

where $E = X_d - X$, and $h(q,\dot{q}) = C(q,\dot{q})q + G(q)$.

Equation (15) provides the required input to achieve the desired impedance (14). Notice that the convergence is defined around the tracking error E, thus the system holds the robot at the reference position X_d at equilibrium.

The impedance control scheme is as shown in Figure 1, where the impedance controller calculates the operational space acceleration a_x according to the kinematic properties of the desired trajectory $\ddot{X}_d$, $\dot{X}_d$, and X_d.

C. The Command Level Redundancy Control

As shown in Fig. 1, the operational space acceleration a_x is derived from the external force and then used by the inverse dynamics controller to compute the required joint space torque, τ. It is possible at this point to insert a null space projector to exclude the force component that project into the null space, in this case the components that moves the remote center of motion away from the entry point. The resultant control would than prevent the remote center of motion from moving.

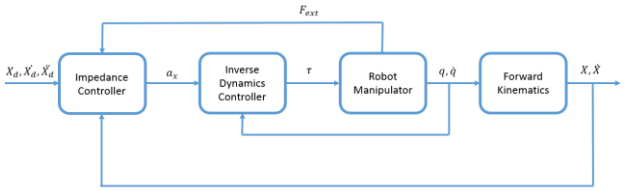

Figure 1. The implementation of the dynamic based impedance control

III. SMALL MASS MODEL FOR COMPLIANCE CONTROL

With the impedance control to realize the mass effect, one can already drag the robot around with ease. It is proper at this point to discuss the nature of the operation. Of success operation, it is nature for the robot to exhibit maximum flexibility. Thus, one desires very small effective mass with very soft reaction force from the robot. As described in [11], the admittance control is more suitable for stiff environment but the impedance control is more suitable for soft contact with small impedance. This is also partly the reason why this research has adopted impedance control. Again, both the impedance control and the admittance control, i.e. the compliance control, effectively recognize position input for reference.

A. The Small Mass Model Formulation

With the impedance control setup provided in the previous sections in mind, the design is to achieve the mass damper effect as

$$M\ddot{X}_n + B\dot{X}_n = {}^wF_n \qquad (16)$$

Subscript n in the above equation indicates the sampling instance, and M and B are the desired effective mass, which would be as small as possible, and damping. ${}^wF$ in (16) is the applied force vector in the world coordinates. The relationship can be decoupled into the respective axes as:

$$M\ddot{x}_n + B\dot{x}_n = {}^wF_{x\_n} \qquad (17)$$

$$M\ddot{y}_n + B\dot{y}_n = {}^wF_{y\_n}$$

$$M\ddot{z}_n + B\dot{z}_n = {}^wF_{z\_n}$$

In the current scenario, ${}^wF$ could be the touching by the surgeon and the system should sensitively react to it as soon as possible. Yet, it is important not to over react to the stimulation. With the relation (17), it is straight forward to numerically integrate the acceleration and obtain the corresponding x-axis velocity and position as:

$$x_n = \frac{{}^wF_{x_n}\Delta t^2 + (2M + B\Delta t)x_{n-1} - Mx_{n-2}}{M + B\Delta t} \qquad (18)$$

And similarly,

$$y_n = \frac{{}^wF_{y_n}\Delta t^2 + (2M + B\Delta t)y_{n-1} - My_{n-2}}{M + B\Delta t} \qquad (19)$$

$$z_n = \frac{{}^wF_{z_n}\Delta t^2 + (2M + B\Delta t)z_{n-1} - Mz_{n-2}}{M + B\Delta t} \qquad (20)$$

These values are fed to the impedance control for the reference position. Figures 2 and 3 show the simulation results for the effect of the small mass model. Figure 2 show the mass effect. A smaller mass obviously achieves more sensitive response. Basically, with the small mass assigned in the range of testing, the system was able to react to the new position within two seconds.

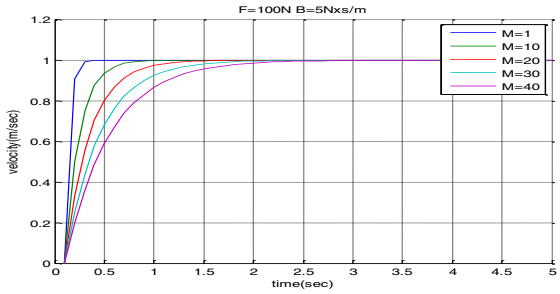

Figure 2. Effect of changing mass in the small mass model

To minimize the speed of the response for less jerk to the surgeon, the effect of changing damping ratio in shown in figure 3. It is desirable to achieve slower response to protect the surgeon. In the figure, one might want to choose a damping ratio higher than 20 to limit the motion speed within 0.5 m/sec.

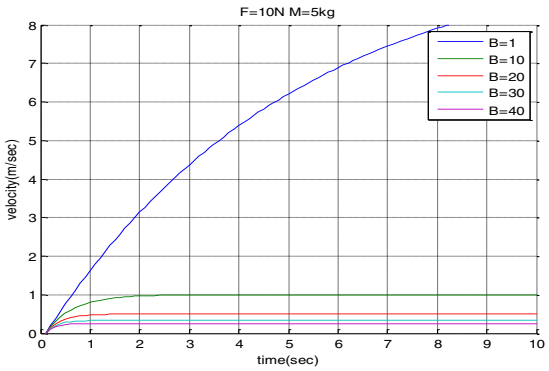

Figure 3. Effect of changing damping ratio in the small mass model

B. *Maintaining the Remote Center of Motion*

From the null space control of the robot arm, the inverse null space projector now acted upon either the velocity loop of the servo system or the acceleration loop of the system. The equation for the impedance control becomes:

$$M\ddot{x}_n + B\dot{x}_n = N_p{}^w F_{x\_n} \qquad (21)$$

$$M\ddot{y}_n + B\dot{y}_n = N_p{}^w F_{y\_n}$$

$$M\ddot{z}_n + B\dot{z}_n = N_p{}^w F_{z\_n}$$

where N_p is the projector matrix to reject the force components that drives the system into the forbidden direction.

C. *Null Space Control in the Arm Servo Controller*

As discussed before, the remote center of motion control can be implemented in the servo controller level. In this case the either the velocity loop or the acceleration loop has to be modified. In this research, we have decided to implement the null space control in the acceleration loop for the simplicity of the formulation.

The

$$\ddot{\boldsymbol{q}}_{\boldsymbol{d}} = \boldsymbol{J}^{\dagger}\left(\ddot{\boldsymbol{X}}_{\boldsymbol{d}} - \dot{\boldsymbol{J}}\dot{\boldsymbol{q}}\right) + (\boldsymbol{I} - \boldsymbol{J}^{\dagger}\boldsymbol{J})\boldsymbol{\xi}_{\boldsymbol{2}} \qquad (22)$$

where $\boldsymbol{\xi}_{\boldsymbol{2}}$ is the acceleration command from the external force. $\boldsymbol{J}(\boldsymbol{q})$ describes the operational space. $\boldsymbol{J}^{\dagger} = \boldsymbol{J}^{\boldsymbol{T}}(\boldsymbol{J}\boldsymbol{J}^{\boldsymbol{T}})^{-\boldsymbol{1}}$ is the pseudoinverse, and $(\boldsymbol{I} - \boldsymbol{J}^{\dagger}\boldsymbol{J})$ projects $\boldsymbol{\xi}_{\boldsymbol{2}}$ onto the null space of the Jacobian $\boldsymbol{J}$ such that $\boldsymbol{\xi}_{\boldsymbol{2}}$ is only effective in the null space and controls the desired acceleration behavior in the null space.

The control schematics becomes

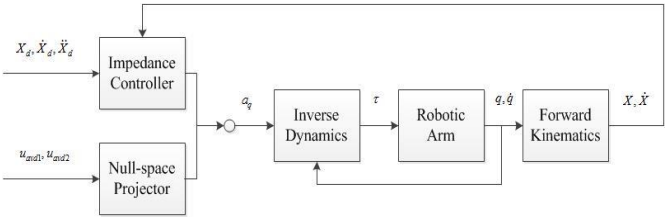

Figure 4. The null-space control implementation

IV. EXPERIMENTAL SETUP

The concept for the implementation is shown in Fig. 3.

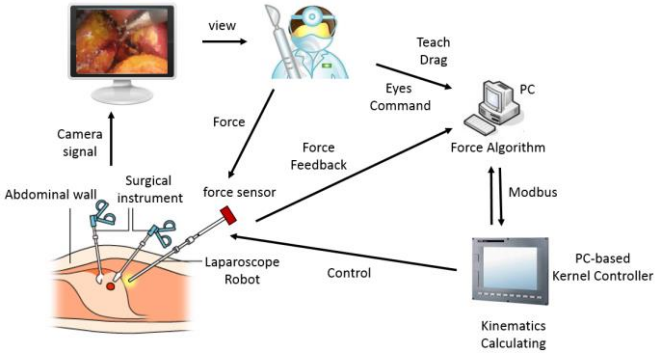

Figure 5. Application scenario for the endoscope holder robot.

As shown in Fig. 5, the endoscope holder holds the endoscope in place through a small fixed opening on the patient. The surgeon may want to change the endoscopic view by touching or pushing the endoscope holder. The robot will then react to the pushing force to achieve the desired attitude.

The robot in this research is a HIWIN RA605 six axes industrial robot. The reason for the industrial is purely for the economic purpose. The robot is actually a donation from the SYNTEC Technology Co., LTD., Taiwan. Because it is an industrial robot, it uses three AC power. The axis motors are AC servo motor with breaks and with reduction gear trains. The axes motors are from FRLS series AC servo motors from HIWIN MIKROSYSTEM. The servo motors are equipped with 17bits absolute position and with serial interface. The motor driver is, of course, a 1 KW servo motor driver from SYNTEC CO. There are two 400 W AC motors with rated torque 1.27 Nm and rated current 2.5 A, one 200 W AC servo motor whose rated torque is 0.64 Nm and rated current at 1.92 A, one 100 W AC servo motor for axis four with rated torque at 0.32 Nm

and rated current at 0.9 A. The motors for axes five and six are two 50 W AC servo motor with rated 0.16 Nm torque and 0.9 A rated current. The servo motors are each equipped with minimum backlash reduction gear box to enhance on the torque output and angular resolution. The end effector of the robot is then fitted with a six axes load cell capable of sensing three axes forces and three axes moments.

This research also used a SYNTEC F11-21R-A-10 complex robot controller. The controller is equipped with 1 GHz clock processor capable of floating point computation for high accuracy forward and inverse kinematic computation. There are many interface ports including serial ports, encoder ports, MPG port, RIO port, Mechatrolink 2 port for Yaskawa servo interface, RS 485, and LAN port. It is a very powerful robot controller with self-sustained forward and inverse kinematic calculation capability.

The implementation schematics is shown in figure 6.

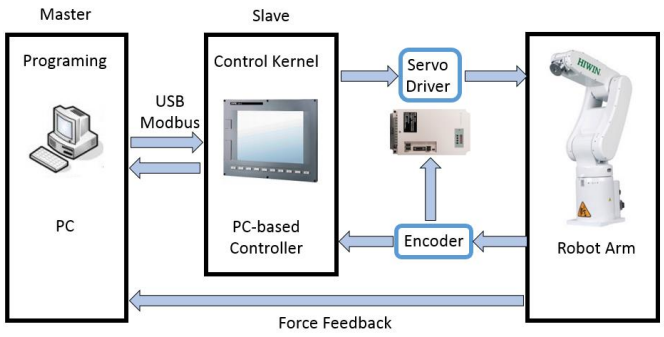

Figure 6. The experimental setup for the endoscope holder system

V. SURGEON AVOIDANCE WITH FIXED ENDOSCOPE ENTRY POSITION

Examining the kinematic design of the robot, the first three axes affect the translational position of the end effector while the last three axes achieve the desired attitude of the end effector. Understanding this basic kinematic structure helps realizing the partially constraint motion of the robot holder.

As a first step, consider the case when one would like to move the robot arm around while keeping the endoscope at a fixed attitude. The procedure is to decompose the applied force into six axes actuation signals. In this case, the system first neglect the torque components, and take the three force components, ${}^{6}F_x$, ${}^{6}F_y$, ${}^{6}F_z$, and convert them into the earth coordinates, ${}^{w}F_x$, ${}^{w}F_y$, ${}^{w}F_z$. Notice that the load cell is mounted on the end of the robot holder and the measurement is thus in line with the coordinates of sixth axis. The force components can then be associated with the input to the small mass model for impedance control. Notice that the forces do not exert rotational motion in the earth coordinates, the attitude of the endoscope is held constant.

When the surgeon touches the endoscope holder, the robot should move to avoid the surgeon while maintaining the remote center of motion. In this case, the procedure is more involved. First the system calculates the torque components induced by the touching force, ${}^{6}M_x$, ${}^{6}M_y$, ${}^{6}M_z$. These torque components are again converted into the earth coordinates, ${}^{w}M_x$, ${}^{w}M_y$, ${}^{w}M_z$ through Euler rotational transformation. Through a similar process as in section 4 for angular motion, it is possible to again calculate for the reference angular position references, θ_{Mx}, θ_{My}, and θ_{Mz} from the small mass model. The reference Euler angle then serves as the reference angular position for the impedance control.

Figure 7 show the actual experimental setup. The cardboard box represents the patient body. The endoscope goes through the small hole on the box and the location of the hole is fixed. When someone touches the endoscope holder, the load cell at the end of the holder will sense the touching force and sends the data to the control computer for processing. The control computer executes the rotational transformation to separate the forces from the applied torque. The force and torque results are then send to the impedance controller. The SYNTEC F11-21R-A-10 robot controller is capable of the forward and inverse kinematic calculation, thus the control computer only needs to compute the desired location and attitude of the arm and the robot controller took over the rest of the control task. Notice the Scotch tape used to hold the box, there is very little or no literal force exerted on the box when the endoscope holder is in the fixed position mode. Figure 8 shows the results of the fixed point control when the endoscope holder is pushed in the *x*-axis direction. One see that the location of the endoscope is held fixed in the upper half of figure 8 while the attitude (A, B, C represent the ZXZ attitude of the Euler transformation) changes. To save space, the similar result for pushing the robot in the *y*-axis is not shown here. Figure 9 shows the result when using the null-space control in the servo loop. One see that the algorithm is still able to maintain the constant remote center of motion position However, there were more oscillation observed in the response. This could be due to the fact that the control is now embedded within the servo loop and is thus much faster than the control in the command level. As a result, it is also more responsive to the disturbance signal.

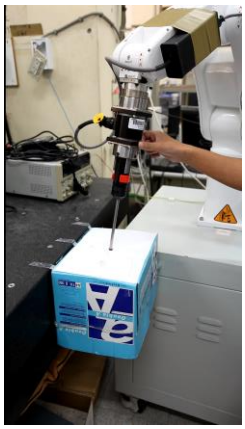

Figure 7. Endoscope holder experiment setup

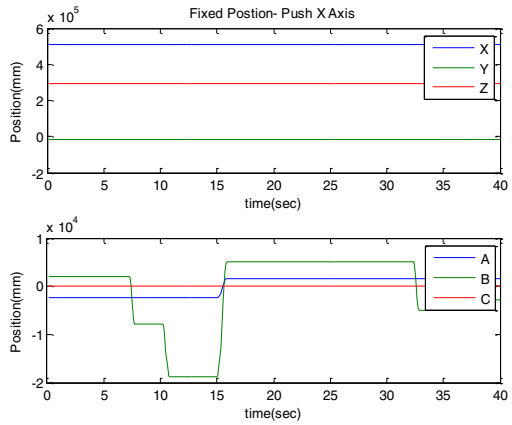

Figure 8. Test results for the fixed point holding experiment while pushing the robot in the *x*-axis direction

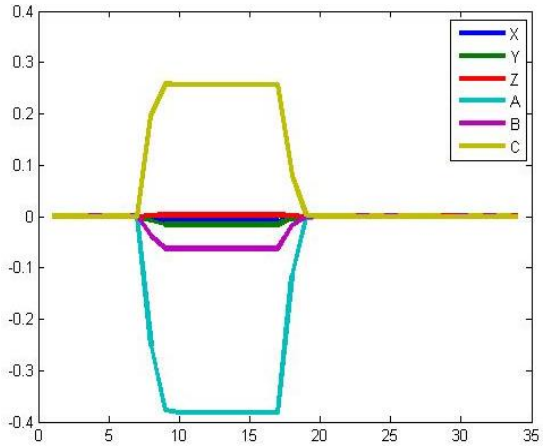

Figure 9. Impedance control in conjunction to the null space control

VI. Conclusion

This research investigates the control of an endoscope holder robot. Unlike the conventional compliance controlled robot, the endoscope holder robot not only has to move according to the drag and push force applied by the user, but also has to hold the entry opening position in place. To achieve this purpose, this research proposes to decouple the control goals. An impedance control first holds the endoscope in place through the MIS opening. The pushing force is sensed by a very sensitive sex-axes load cell. Experimental results showed that both controls were effective. The null space control is somewhat more oscillatory maybe due to the faster response and also due to the lower level implementation which cause the robot arm to response to more of the disturbance signals.

References

[1] B. S. Peters, P. R. Armijo, C. Krause, S. A. Choudhury, and D. Oleynikov, "Review of emerging surgical robotic technology," *Surgical Endoscopy and Other Interventional Techniques,* Article in Press pp. 1-20, 2018.

[2] I. Intuitive Surgical. (2016, 10/28). *The da Vinci Surgical System*. Available: http://www.davincisurgery.com/da-vinci-surgery/da-vinci-surgical-system/

[3] J. T. Wilson, T. C. Tsao, J. P. Hubschman, and S. Schwartz, "Evaluating remote centers of motion for minimally invasive surgical robots by computer vision," in *IEEE/ASME International Conference on Advanced Intelligent Mechatronics, AIM*, 2010, pp. 1413-1418.

[4] J. Y. K. Chan *et al.*, "Foot-controlled robotic-enabled endoscope holder for endoscopic sinus surgery: A cadaveric feasibility study," *Laryngoscope,* Article vol. 126, no. 3, pp. 566-569, 2016.

[5] Y. He, P. Zhang, H. Jin, Y. Hu, and J. Zhang, "Type Synthesis for Remote Center of Motion Mechanisms Based on Coupled Motion of Two Degrees-of-Freedom," *Journal of Mechanical Design, Transactions of the ASME,* Article vol. 138, no. 12, 2016, Art. no. 122301.

[6] L. Zorn *et al.*, "A Novel Telemanipulated Robotic Assistant for Surgical Endoscopy: Preclinical Application to ESD," *IEEE Transactions on Biomedical Engineering,* Article in Press 2017.

[7] M. N. Rahman and R. K. Mishra, "The camera-holding robotic device in laparoscopy surgery," *World Journal of Laparoscopic Surgery,* Review vol. 4, no. 3, pp. 132-135, 2011.

[8] B. Cabuk, S. Ceylan, I. Anik, M. Tugasaygi, and S. Kizir, "A haptic guided robotic system for endoscope positioning and holding," *Turkish Neurosurgery,* Article vol. 25, no. 4, pp. 601-607, 2015.

[9] J. M. Gilbert, "The EndoAssist™ robotic camera holder as an aid to the introduction of laparoscopic colorectal surgery," *Annals of the Royal College of Surgeons of England,* Article vol. 91, no. 5, pp. 389-393, 2009.

[10] K. Zinchenko, C. Y. Wu, and K. T. Song, "A study on motion control of a robotic endoscope holder using speech recognition," in *Proceedings of the IEEE International Conference on Industrial Technology*, 2016, vol. 2016-May, pp. 1472-1475.

[11] A. Calanca, R. Muradore, and P. Fiorini, "A review of algorithms for compliant control of stiff and fixed-compliance robots," *IEEE/ASME Transactions on Mechatronics,* Article vol. 21, no. 2, pp. 613-624, 2016, Art. no. 2465849.

[12] N. Hogan, "IMPEDANCE CONTROL: AN APPROACH TO MANIPULATION: PART I - THEORY," *Journal of Dynamic Systems, Measurement and Control, Transactions of the ASME,* Article vol. 107, no. 1, pp. 1-7, 1985.